Reduced Complexity Receivers for Layered Space–Time CPM

Wanlun Zhao, *Student Member, IEEE,* and Georgios B. Giannakis, *Fellow, IEEE*

***Abstract*—Layered space–time (LST) transmissions employing continuous phase modulations (CPM) are well motivated for both bandwidth- and power-limited multiantenna communications. However, one of the major challenges for LST-CPM is the high complexity it incurs with maximum likelihood (ML) detection. In this paper, we develop reduced complexity LST-CPM receivers. First, we consider single antenna systems. Specifically, we study a reduced complexity Viterbi receiver for binary CPM. Based on this design, we introduce differential encoding for a class of CPM signals and analyze its performance gain both theoretically and with simulations. Second, we focus on multiantenna LST systems with minimum shift-keying (MSK)-type modulations. With group nulling-canceling (NC) and low-complexity linear equalization, we convert a coded multiuser detection problem into an uncoded one with small equalization loss. We also find that the combination of sphere decoding with hard-decision iterative processing is effective in boosting performance with a controllable complexity increase. Both analytical and simulated performance confirm that the novel LST-MSK receiver exhibits markedly improved performance relative to conventional NC detectors with moderate complexity increase.**

***Index Terms*—Continuous phase modulation (CPM), fading channel, minimum shift keying (MSK), multiuser detection, performance analysis, space time.**

I. Introduction

CONTINUOUS phase modulation (CPM) has long been recognized to possess many desirable features for communication systems that are both bandwidth and power limited [2], [10]. Due to their phase continuity, CPM signals exhibit relatively lower spectral side lobes than signals with abrupt phase changes. Their compact spectra enable CPM signals to be efficiently multiplexed. Furthermore, CPM waveforms are constant modulus, which allows nonlinear high-power amplifiers to operate efficiently. Nonetheless, CPM transmissions incur high maximum likelihood (ML) decoding complexity. Many matched filters have to be implemented at the receiver front end, and Viterbi's algorithm with possibly a large number of states has to be employed. Valuable in designing simplified receivers is Laurent's decomposition, where binary CPM is represented by a linear superposition of a finite number of amplitude modulated pulses [8]. Laurent's decomposition was extended to M-ary CPM in [9], but except for the binary case, it has found limited applicability to reduced complexity designs [8], [9]. A simplified decision rule was derived for binary CPM, and a receiver example for Gaussian minimum shift keying (GMSK) was provided [7]. We first review the simplified receiver structure that was suggested and introduce differential encoding for a class of CPM signals, in order to improve performance of coherent detection.

Recent information theoretic results show that multiantenna channels offer the potential for enhanced capacity relative to their single-antenna counterparts [5], [15]. Going well beyond the aforementioned single-antenna CPM extensions, the main focus of this paper is on multiantenna layered space–time (LST) CPM systems, which we naturally term LST-CPM. In such systems, CPM features constant modulus and compact spectra, while ST multiplexing offers increased capacity in a rich scattering environment. LST-CPM is thus an attractive choice for both power and bandwidth-limited multiantenna systems. However, the high complexity of ML demodulation of LST-CPM poses a greater challenge than the single-antenna case. Due to self-interference among simultaneously transmitted waveforms, the ML detection complexity is generally high for LST systems even with linear modulations. Receivers for complex CPM transmissions make the problem worse. This motivates our emphasis on reduced complexity LST-CPM receiver structures. Specifically, we will focus on a novel receiver design for LST systems employing MSK-type modulations, which efficiently exploits the structure of MSK along with intermediate sphere decoding results to facilitate the hard-decision iterative decoding process.

There are several related works on ST-CPM. Design criteria were introduced for ST-CPM to enable full transmit and receive antenna diversity in [20], where the emphasis was on error performance rather than low complexity receivers. An orthogonal structure was imposed on the transmitted waveforms to reduce ML detection complexity for a two transmit antenna system in [17], but even in this case complexity is still high for bandwidth efficient partial response CPM. A soft decision iterative receiver with joint channel estimation and symbol detection was derived for ST-CPM in [19]. Different from existing works, we consider LST (BLAST-type) systems with a large number of transmit and receive antennas. BLAST systems were considered in, e.g., [4] and [14], but only for linear modulations. They often do not invoke ST coding to enable transmit diversity but rely on the receive diversity to achieve the required performance.

The organization of the paper is as follows. In Section II, the decomposition of binary CPM is described, and differential encoding for a class of CPM is introduced and justified. In Section III, an LST-MSK-type receiver design is developed and an-

Manuscript received February 26, 2003; revised July 22, 2003 and January 7, 2004; accepted January 22, 2004. The editor coordinating the review of this paper and approving it for publication is A. F. Molisch. This work was supported by the ARO/CTA under Grant DAAD19-01-2-0011. This work was presented in part at the 37th Conference on Information Sciences and Systems (CISS), Baltimore, Maryland, March 12–14, 2003.

The authors are with the Department of Electrical and Computer Engineering, University of Minnesota, Minneapolis, MN 55455 USA (e-mail: wlzhao@ece.umn.edu; georgios@ece.umn.edu).

Digital Object Identifier 10.1109/TWC.2004.843051

1536-1276/$20.00 © 2005 IEEE

alyzed. In Section IV, simulation results of our LST-MSK-type receiver are shown. Finally, conclusions are drawn in Section V.

Notation: Upper (lower) boldface letters denote matrices (column vectors); $(\cdot)^T$ and $(\cdot)^H$ denote transpose and Hermitian, respectively; $\delta_{i,j}$ and $\delta(t,\tau)$ represent the Kronecker delta and Dirac delta, respectively; $\Re(\cdot)$ and $\Im(\cdot)$ denote the real and imaginary parts; $\|\cdot\|$ represents the Frobenius norm; $\mathbb{N}$ stands for the set of natural numbers; $\mathcal{N}(\cdot,\cdot)$ and $\mathcal{CN}(\cdot,\cdot)$ represent the real and complex Gaussian distributions; $\mathcal{Q}(x)$ is the Gaussian $\mathcal{Q}$ function; $\mathbf{I}$ and $\mathbf{0}$ denote the identity and all-zero matrices, except when explicitly defined otherwise.

II. Single-Antenna Binary CPM

CPM transmissions are, in general, nonlinear functions of the information-bearing sequence. However, it was shown in [8] that any binary CPM signal can be exactly represented as a linear superposition of a finite number of amplitude modulated pluses. Furthermore, it was observed that only a few modulated pulses are needed to accurately approximate a binary CPM signal, which forms the basis of simplified receiver designs. We will review this decomposition next.

A. Decomposition of Binary CPM

A complex baseband binary CPM signal can be represented as [2]

$$\begin{aligned} s(t) &= \sqrt{\frac{2E}{T}}\exp(j\phi(t)), \quad t = nT+\tau,\ 0<\tau<T \\ \phi(t) &= \pi h \int_0^t \sum_k b_k g(\tau - kT)d\tau \\ &= \pi h \sum_{k=0}^{n} b_k q(t-kT) \end{aligned} \tag{1}$$

where E is the transmitted bit energy, T is the symbol period, h is the modulation index, $\{b_k\}$ is the sequence of independent information symbols drawn from ± 1, $g(t)$ is the spectral shaping pulse with $g(t) \neq 0$ only when $0 < t < LT$, and $q(t) := \int_0^t g(\tau)\, d\tau$ is the phase smoothing response with $q(t) = 1$, for $t \geq LT$. Clearly, the phase $\phi(t)$ is a continuous function of time. If $L = 1$, $s(t)$ is called full response CPM, whereas if $L > 1$, $s(t)$ is referred to as partial response CPM. It turns out that the smoother the pulse $g(t)$ is, the more spectrally efficient CPM is [2]. In practice, smooth pulse shapers, such as Gaussian or raised cosine pulses, are often used. When $h = 1/2$, binary CPM is referred to as MSK-type modulation.

An equivalent representation of the binary CPM waveform in terms of K pulse components $\{c_k(t)\}_{k=0}^{K-1}$ is [8]

$$s(t) = \sqrt{\frac{2E}{T}} \sum_{n=0}^{\infty} \sum_{k=0}^{K-1} a_{k,n} c_k(t-nT) \tag{2}$$

where $K := 2^{L-1}$ denotes the total number of pulse components needed to represent $s(t)$, and the coefficients $\{a_{k,n}\}_{k=0}^{K-1}$ depend on the information sequence $\{b_n\}$ as follows:

$$a_{k,n} = \exp\left(j\pi h \left[\sum_{i=0}^{n} b_i - \sum_{i=1}^{L-1} b_{n-i}\alpha_{k,i}\right]\right) \tag{3}$$

TABLE I
Pulse Component Length

$c_0(t)$	$(L+1)T$
$c_1(t)$	$(L-1)T$
$c_2(t),\ c_3(t)$	$(L-2)T$
$\dots$	$\dots$
$c_{K/2}(t),\dots,c_{K-1}(t)$	T

with $\alpha_{k,i}$s denoting the bits in the binary representation of k. That is, $k = \sum_{i=1}^{L-1} 2^{i-1}\alpha_{k,i}$ with $\alpha_{k,i} \in \{0,1\}$. Generally, $\{a_{k,n}\}$ are nonlinear functions of $\{b_n\}$, which captures the nonlinear nature of CPM. To specify the pulses in (2), we need two additional definitions

$$\beta(t) := \begin{cases} \pi h q(t) & 0 \leq t \leq LT \\ \pi h[1 - q(t-LT)] & LT \leq t \leq 2LT \end{cases}$$

and $\gamma_n(t) := \sin[\beta(t+nT)]/\sin(\pi h)$. Using these definitions, we can express $c_k(t)$ as

$$c_k(t) = \gamma_0(t) \prod_{i=1}^{L-1} \gamma_{i+\alpha_{k,i}L}(t).$$

The duration of $c_k(t)$ is nonincreasing with k (see Table I), and the signal energy conveyed by $c_k(t)$ decreases drastically with the pulse duration. The decomposition in (2) does not apply when h takes integer values, but bandwidth efficient CPM typically corresponds to $h < 1$.

It turns out that $c_0(t)$ is the pulse with the longest duration, which also carries most of the signal energy [8]. For example, in the decomposition of GMSK with $L = 4$ and $BT = 1/4$, where B is the 3-dB bandwidth of $g(t)$, $c_0(t)$ has length $5T$ and carries 0.991 944 of the signal energy, $c_1(t)$ has length $3T$ and carries 0.008 03 of the energy, while the remaining six pulses only contain 2.63×10^{-5} (-45.8 dB) of the total energy [7]. Exploiting the fact that binary CPM signal can be accurately approximated with only a few pulse components in the linear decomposition (2), a simplified decoder was derived in [7].

B. Minimum Trellis for Simplified Viterbi Receivers

It is well known that the optimum Viterbi receiver for binary CPM with pulse $g(t)$ of duration LT and modulation index $h = m/p$, where m and p are coprime, entails a $p2^{L-1}$-state phase trellis [10], [11]. With $L > 1$, partial response CPM has desirable spectral characteristics: a narrow main lobe and fast rolling-off side lobes. However, the ML detection complexity increases exponentially with L.

To reduce the complexity, we will use only $P < K$ components in the Viterbi decoder. The received signal in additive white Gaussian noise (AWGN) is

$$y(t) = s(t) + n(t) = \tilde{s}(t) + e(t) + n(t), \quad 0 \leq t \leq NT$$

where $s(t)$ is the transmitted binary CPM waveform in (2); $n(t)$ is the zero mean AWGN with $\mathbf{E}[n(t)n^*(\tau)] = N_0\delta(t,\tau)$; $\tilde{s}(t)$ is the P-component approximation of $s(t)$ defined as $\tilde{s}(t) = \sqrt{2E/T}\sum_{n=0}^{N-1}\sum_{k=0}^{P-1} a_{k,n}c_k(t-nT)$; and $e(t)$ is the

approximation error. Neglecting the signal energy conveyed by $\{c_k(t)\}_{k=P}^{K-1}$, the simplified decision rule is [7]

$$\{\hat{b}_n\}_{n=0}^{N-1} = \arg \max_{\{b_n\}_{n=0}^{N-1}} \Re(y(t), \tilde{s}(t)) = \arg \max_{\{b_n\}_{n=0}^{N-1}} \sum_{n=0}^{N-1} \sum_{k=0}^{P-1} \Re(y_{k,n} a_{k,n}^*) \quad (4)$$

where $(x(t), y(t)) := \int_0^{NT} x(t) y^*(t) dt$ denotes the inner product of $x(t)$ and $y(t)$, $y_{k,n} := \int y(t) c_k(t - nT)\, dt$, and $\tilde{s}(t)$ and $a_{k,n}$s are completely determined by $\{b_n\}_{n=0}^{N-1}$. It can be observed from (4) that the coefficients $\{a_{k,n}\}_{n=0}^{N-1}$, instead of $\{b_n\}_{n=0}^{N-1}$, are directly involved in the metric calculation. Furthermore, $\{b_n\}_{n=0}^{N-1}$ can be uniquely determined by $\{a_{0,n}\}_{n=0}^{N-1}$.

The minimum trellis of the Viterbi receiver is specified next. To determine the minimum number of states for the P-component Viterbi receiver, let us examine the memory in $\mathbf{a}_n := [a_{0,n}, \ldots, a_{P-1,n}]^T$. For any P, let L_r be the minimum number of bits needed to represent $P - 1$. It follows from (3) that

$$a_{k,n} = a_{0,n-1} \exp\left(j\pi h \left[b_n - \sum_{i=1}^{L_r} b_{n-i} \alpha_{k,i} \right] \right).$$

Hence, the memory of $\mathbf{a}_n$ is completely determined by $[a_{0,n-1}, b_{n-L_r}, \ldots, b_{n-1}]^T$, which also corresponds to the states of the simplified CPM trellis. Depending on the modulation index $h = m/p$, $a_{0,n-1}$ takes on p values when m is even and $2p$ values when m is odd [10, p. 255]. Defining $\bar{a}_{0,n} := a_{0,n} \exp[j\pi h(n+1)]$, with the tilted phase representation of [11], we can convert a periodic time-varying phase trellis into a time-invariant one. For any $h = m/p$, where m and p are relatively prime, $\bar{a}_{0,n}$ has p states. Finally, at any time instant n, the trellis state is determined by $[\bar{a}_{0,n-1}, b_{n-L_r}, \ldots, b_{n-1}]^T$, and the total number of trellis states becomes $p2^{L_r}$. Furthermore, the state transitions are uniquely determined by (3).

The structure of the simplified Viterbi receiver for binary CPM is shown in Fig. 1, where P matched filters are employed. The P matched filter outputs are sampled every T seconds to obtain the decision statistics $y_{k,n}$. In many practical cases, just $c_0(t)$ and $c_1(t)$ can represent a binary CPM signal with sufficient accuracy. Hence, $L_r = 1$ and a $2p$-state Viterbi receiver is adequate.

C. Differentially Encoded Binary CPM

In this section, differential encoding is introduced for the class of CPM signals with $h = 1/(2Q)$, $Q \in \mathbb{N}$ to annihilate the inherent differential decoding of CPM signals and thus improve error performance for coherent detection. When $h = 1/2$, differentially encoded MSK closely approximates the linearized MSK [13, p. 192].

The block diagram for the differentially encoded binary CPM is depicted in Fig. 2. The information sequence, $\{i_n\}$, $i_n \in \{0, 1\}$, is first differentially encoded to obtain the binary sequence $\{p_n\}$, $p_n \in \{0, 1\}$. Then, $\{p_n\}$ is mapped to the sequence $\{b_n\}$, $b_n \in \{\pm 1\}$, and modulated by binary CPM. It can be easily verified that the sequences $\{i_n\}$ and $\{p_n\}$ have the same mean and correlation functions. Hence, differential

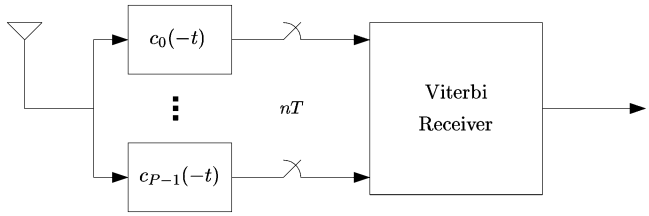

Fig. 1. Simplified Viterbi receiver for binary CPM.

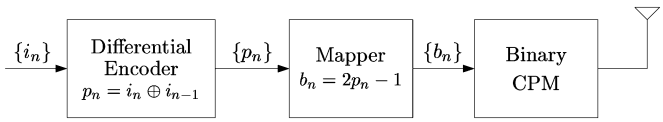

Fig. 2. Differentially encoded binary CPM.

encoding will not alter the desirable spectral characteristics of CPM transmissions.

A simplified Viterbi receiver is used to generate a near-ML sequence estimate for $\{\bar{a}_{0,n}\}$, say $\{\hat{\bar{a}}_{0,n}\}$. Since the sequences $\{i_n\}$ and $\{p_n\}$ have the same statistics, we infer that they will lead to statistically identical error patterns in $\{\hat{\bar{a}}_{0,n}\}$. That is, the error profiles of $\{\bar{a}_{0,n}\}$ are the same for both systems with or without differential encoding. In the following, we examine how to generate the estimate of the information bearing sequence from $\{\hat{\bar{a}}_{0,n}\}$. Without differential encoding, the sequence $\{p_n\}$ in Fig. 2 is considered as the information sequence. Based on $b_n = 2p_n - 1$, the definition of $\bar{a}_{0,n}$ and (3), $\hat{p}_n$ is determined by solving $\exp[j\,\pi\, h\,(2\hat{p}_n - 1)] = \hat{\bar{a}}_{0,n} \hat{\bar{a}}_{0,n-1}^*$. It is clear that there is an inherent differential decoding in the detection process. Since two symbols, $\bar{a}_{0,n}$ and $\bar{a}_{0,n-1}$, are involved in the detection of p_n, a single error in $\{\hat{\bar{a}}_{0,n}\}$ may cause two errors in $\{\hat{p}_n\}$, which results in performance degradation. Let us now consider the case with differential encoding. This time, our goal is to find $\{\hat{i}_n\}$ from $\{\hat{\bar{a}}_{0,n}\}$. Since the introduced differentially encoded CPM works only for a special set of modulation indexes, we henceforth consider $h = 1/(2Q)$, $Q \in \mathbb{N}$. Following (3), we can determine x_n from $\hat{\bar{a}}_{0,n}$ using $\pi h \sum_{i=0}^{n} (b_i + 1) = x_n + 2k\pi$, where $x_n \in \{0, 2\pi h, \ldots, (2Q-1)2\pi h\}$. Letting $y_n := x_n/(2\pi h)$, and since $b_n = 2p_n - 1$, it follows that $\sum_{i=0}^{n} p_i = y_n + 2kQ$, $y_n \in \{0, 1, \ldots, 2Q-1\}$. The estimate of the input bit can be obtained by $\hat{i}_n = (y_n)_{\mathrm{mod}2}$, where the equality follows from the fact that

$$\left(\sum_{i=0}^{n} p_i \right)_{\mathrm{mod}2} = (i_n \oplus i_{n-1}) \oplus \cdots \oplus (i_0 \oplus 0) = i_n.$$

From this derivation, we observe that $\hat{i}_n = f(\hat{\bar{a}}_{0,n})$, where f is, in general, a nonlinear function of $\hat{\bar{a}}_{0,n}$. That is, $\hat{i}_n$ depends on $\hat{\bar{a}}_{0,n}$ only. This differential encoding for binary CPM can be generalized to M-ary CPM with M-ary differential encoding. We have noticed that for $h = 1/(2Q)$, differential encoding is applicable to M-ary CPM, where $M \geq 2$ is an integer factor of $2Q$. For example, when $h = 1/8$, this differential encoding is applicable to $M = 2, 4, 8$.

Let us now analyze the performance improvement of the introduced differential encoding in AWGN. It is well known that the single most important parameter characterizing the symbol

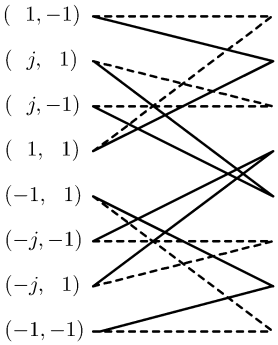

Fig. 3. Eight-state trellis for binary CPM with $h = 0.25$.

error probability at high signal-to-noise ratio (SNR) is the minimum Euclidean distance ($d_{\min}$) [2]. For binary CPM with small modulation indexes, $d_{\min}$ is calculated as [2]

$$d^2_{\min} = \frac{1}{T}\int_0^{(L+1)T} [1 - \cos\varphi(t)]dt$$

where

$$\varphi(t) = \begin{cases} 2\pi h q(t) & 0 \le t \le T, \\ 2\pi h[q(t) - q(t-T)] & T \le t \le (L+1)T. \end{cases}$$

$\varphi(t)$ is the corresponding phase difference between any two input sequences $\{b_n\}$ that achieves the minimum Hamming distance, say $\{\ldots, 1, -1, \ldots\}$ and $\{\ldots, -1, 1, \ldots\}$. It is clear that an error event that achieves $d^2_{\min}$ results in two errors in $\{b_n\}$ and hence in $\{p_n\}$. On the other hand, since $a_{0,n} = \exp(j\pi h \sum_{i=0}^{n} b_i)$, this error event results in only one error in $\{a_{0,n}\}$, hence one error in $\{i_n\}$. We have observed from simulations that the number of errors without differential encoding is approximately twice that with differential encoding.

D. Design Example

As a design example, we consider binary partial response CPM with modulation index $h = 1/4$. We use a truncated Gaussian pulse $g(t)$ with $L = 4$ and $BT = 1/4$, which has excellent spectral characteristics. For conventional ML decoding, a 32-state Viterbi receiver is needed. On the other hand, the simplified Viterbi receiver based only on the first two pulse components has eight states. Since $\bar{a}_{0,n} = \exp(\pi/4 \sum_{i=0}^{n}(b_i + 1))$, it is clear that $\bar{a}_{0,n} \in \{\pm 1, \pm j\}$. The eight-state trellis is shown in Fig. 3, where the solid lines correspond to the new input $b_n = 1$, whereas the dashed lines correspond to $b_n = -1$.

The bit-error rate (BER) performance of binary CPM with $h = 1/4$ and $h = 1/2$ are depicted in Fig. 4 along with the BER curves of their differentially encoded counterparts. An eight-state and a four-state Viterbi receiver is employed for $h = 1/4$ and $h = 1/2$, respectively. We can observe that for both indexes, performance gains are achieved throughout the entire SNR range. In Fig. 4, the performance for a linear GMSK receiver is also shown, which will be addressed later.

III. LST Binary CPM

In this section, we shift focus to the multiantenna LST-CPM, and our goal is to design reduced complexity LST-MSK-type receivers. We will start with the channel and system models and move on to derive sufficient statistics for LST-CPM, before deriving and analyzing our LST-MSK receiver designs.

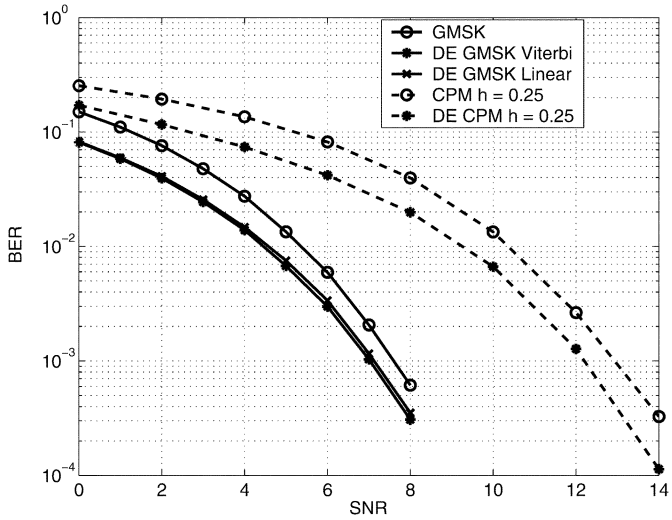

Fig. 4. BER performance gain of differentially encoded CPM with $h = 1/2$ and $h = 1/4$.

A. Channel and System Modeling

Consider a coherent space–time communication system with N_t transmit and $N_r \ge N_t$ receive antennas. The channels between different transmit and receive antennas are assumed to be mutually independent, quasistatic, and flat Rayleigh faded. Let $\mathbf{H}$ be the fading channel coefficient matrix with (μ, ν)th entry and $h_{\mu,\nu}$ denoting the channel coefficient from the νth transmit to the μth receive antenna. Then, $h_{\mu,\nu}$ is complex Gaussian distributed with zero mean and unit variance; i.e., $h_{\mu,\nu} \sim \mathcal{CN}(0,1)$, $\mu \in \{1, \ldots, N_r\}$, $\nu \in \{1, \ldots, N_t\}$. The matrix $\mathbf{H}$ remains invariant during the channel's coherence interval of length NT but is allowed to vary independently from block to block. Perfect knowledge of each channel realization is assumed only at the receiver end.

We suppose that the receive diversity is sufficient to provide required performance. No additional space–time coding is employed. Each transmit antenna sends its own binary CPM signals independently. That is, during a block length of NT, the $N \times 1$ binary information vectors $\mathbf{i}_1, \mathbf{i}_2, \ldots, \mathbf{i}_{N_t}$ are differentially encoded, modulated by binary CPM, and transmitted simultaneously via the N_t transmit antennas. The continuous time data model is

$$\mathbf{y}(t) = \mathbf{H}\mathbf{s}(t) + \mathbf{n}(t), \quad 0 \le t \le NT \tag{5}$$

where $\mathbf{y}(t) := [y_1(t), y_2(t), \ldots, y_{N_r}(t)]^T$, $\mathbf{s}(t) := [s_1(t), s_2(t), \ldots, s_{N_t}(t)]^T$, and $\mathbf{n}(t) := [n_1(t), n_2(t), \ldots, n_{N_r}(t)]^T$. In the definition of $\mathbf{s}(t)$, $s_\nu(t)$ is the continuous phase waveform corresponding to $\mathbf{i}_\nu$, $y_\mu(t)$ is the received waveform at the μth receive antenna, and $n_\mu(t)$ is the zero mean AWGN at the μth receive antenna with $E[n_\mu(t)n^*_\nu(\tau)] = N_0\delta_{\mu,\nu}\delta(t,\tau)$.

It follows readily from (5) that the ML decision rule is

$$\hat{\mathbf{I}}_{ML} = \arg\max_{\mathbf{I}} \sum_{\mu=1}^{N_r} \Re(y_\mu(t), \sum_{\nu=1}^{N_t} h_{\mu,\nu} s_\nu(t)) \tag{6}$$

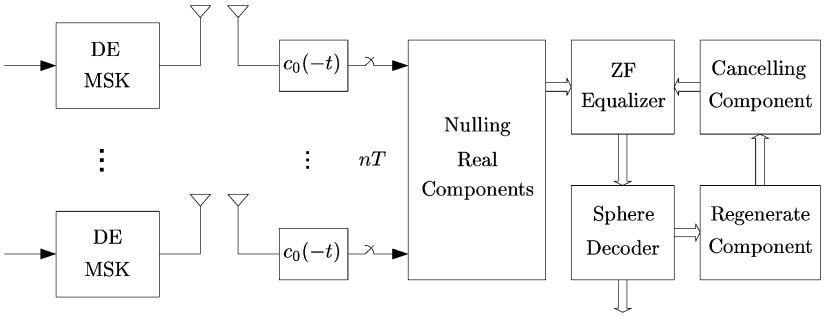

Fig. 5. Simplified LST-MSK-type system.

where $\mathbf{I} := [\mathbf{i}_1, \mathbf{i}_2, \ldots, \mathbf{i}_{N_t}]$ denotes the possible transmitted information matrix, and $s_\nu(t)$s are completely determined by $\mathbf{I}$. With the binary CPM decomposition in (2), we can express (6) as

$$\hat{\mathbf{I}}_{ML} = \arg\max_{\mathbf{I}} \Re \sum_{n=0}^{N-1} \sum_{\mu=1}^{N_r} \sum_{\nu=1}^{N_t} h^*_{\mu,\nu} \sum_{k=0}^{K-1} a^*_{k,n,\nu} y_{k,n,\mu} \quad (7)$$

where $y_{k,n,\mu} := \int y_\mu(t) c_k(t - nT)\, dt$. The sufficient statistics are $y_{k,n,\mu}$, $k \in \{0, \ldots, K-1\}$, $n \in \{0, \ldots, N-1\}$, and $\mu \in \{1, \ldots, N_r\}$. To generate all these decision statistics, K matched filters have to be used per receive antenna. To implement the ML decision rule in (7), an optimal detector employing the Viterbi algorithm must search through a $(p\, 2^{L-1})^{N_t}$ state trellis, which has prohibitively high complexity, even when N_t and L are moderate.

It has been shown in [11] that any CPM can be viewed as the concatenation of a continuous phase encoder (CPE) and a memoryless mapper (MM). CPE is essentially a trellis encoder. From this decomposition of CPM, and our assumption of independent transmissions from the N_t transmit antennas, LST-CPM detection boils down to the mathematical model of a coded multiuser detection problem. For recent advances in this problem, the interested readers are referred to [3] and the references therein. To achieve near-ML performance with feasible complexity, these recent results favor soft decision iterative processing [3]. However, the complexity of soft decision iterative detection is still very high. Next, we will show how this complexity can be reduced for a practical class of LST-CPM transmissions.

B. Reduced Complexity LST-MSK Receivers

MSK-type modulations form a special class in binary CPM and find wide-spread applications. In particular, Gaussian MSK has been adopted by many standards, such as GSM, DECT, and Bluetooth. In this section, the design insight behind the conventional parallel-type MSK linear receiver is described first [2], [7]. A reduced-complexity suboptimal LST-MSK receiver is developed subsequently. A single-pulse approximation for MSK-type modulations and the MSK-type linear receiver will be employed in our novel LST receiver design.

We focus on a differentially encoded partial response MSK-type system. The one pulse approximation of MSK is $\tilde{s}(t) = \sqrt{2E/T} \sum_{n=0}^{\infty} a_{0,n} c_0(t - nT)$, where $a_{0,n}$ is defined in (3) with $a_{0,2n-1} \in \{\pm 1\}$, and $a_{0,2n} \in \{\pm j\}$. The memory in $\tilde{s}(t)$ is due to $c_0(t)$ only, since the duration of $c_0(t)$ is $(L+1)T$ and $E[a_{0,n} a^*_{0,k}] = \delta_{n,k}$. This memory of $\tilde{s}(t)$ can be viewed as controlled intersymbol interference (ISI) introduced by the modulator. Furthermore, notice that independent binary symbols are carried alternately by the in-phase and quadrature components. With perfect separation of these two components, ISI in each one of them is less severe, allowing for low complexity linear equalization techniques to effectively reduce the mild ISI per branch. This key observation forms the basis of the conventional MSK-type receivers. We apply this design to the differentially coded GMSK. The small performance loss of this linear receiver compared to a four-state Viterbi receiver is illustrated in Fig. 4. It can be observed that the one pulse approximation of GMSK incurs a tolerable error performance degradation.

Equipped with design insights from conventional MSK-type receivers, we now proceed to design LST-MSK transceivers. The block diagram for our LST-MSK system is shown in Fig. 5. Differentially encoded partial response MSK-type modulation is employed at the transmitter. One-pulse approximation is adopted. Hence, only one matched filter, $c_0(-t)$, is used per receive antenna. The outputs of the matched filters are sampled every T seconds to generate the decision statistics. The simplified discrete-time baseband equivalent model to (5) is therefore

$$\mathbf{y}_n = \mathbf{H}\mathbf{s}_n + \mathbf{w}_n, \quad n = 0, \ldots, N-1 \quad (8)$$

where $\mathbf{y}_n := \int \mathbf{y}(t) c_0(t - nT) dt$, $\mathbf{s}_n := \int \mathbf{s}(t) c_0(t - nT) dt$, and $\mathbf{w}_n := \int \mathbf{n}(t) c_0(t - nT) dt$. Since the duration of $c_0(t)$ is $(L+1)T$, successive $\mathbf{w}_n$s are correlated. However, at time index n, $\mathbf{w}_n \sim \mathcal{CN}(\mathbf{0}, \|c_0\|^2 N_0 \mathbf{I})$, since the noise components at different receive antennas are independent.

Under the block fading assumption, signals from different transmit antennas share the same known ISI structure. However, direct multichannel equalization causes a large performance loss. Our idea to reduce this loss is to apply array processing techniques to separate real and imaginary components into two groups. Low complexity linear equalization can then be applied to reduce ISI in each group. This converts the coded multiuser detection problem into an uncoded one. For practical N_t and N_r values, say less than 15, lattice search algorithms, such as sphere decoding, can be used to solve the uncoded multiuser detection problem efficiently. The LST-MSK detection process is described in detail next.

First, we briefly describe the group nulling process along the lines of [4] and [14]. The real counterpart of (8) is $\tilde{\mathbf{y}}_n = \tilde{\mathbf{H}}\tilde{\mathbf{s}}_n + \tilde{\mathbf{w}}_n$, where $\tilde{\mathbf{x}} := [\Re\mathbf{x}^T \quad \Im\mathbf{x}^T]^T$, $\mathbf{x}$ can be $\mathbf{y}_n$, $\mathbf{s}_n$ or $\mathbf{w}_n$, and

$$\tilde{\mathbf{H}} = \begin{bmatrix} \Re\mathbf{H} & -\Im\mathbf{H} \\ \Im\mathbf{H} & \Re\mathbf{H} \end{bmatrix}.$$

For convenience, we denote the first N_t columns of $\tilde{\mathbf{H}}$ as $\tilde{\mathbf{H}}_{\Re}$ and the last N_t columns as $\tilde{\mathbf{H}}_{\Im}$. Since $\tilde{\mathbf{H}}$ is almost surely full rank, the null space of $\tilde{\mathbf{H}}_{\Re}$ has dimension $2N_r - N_t$. Let $\{\mathbf{v}_1, \mathbf{v}_2, \ldots, \mathbf{v}_{2N_r-N_t}\}$ be an orthonormal basis for the null space of $\tilde{\mathbf{H}}_{\Re}$. Defining $\mathbf{V} := [\mathbf{v}_1, \mathbf{v}_2, \ldots, \mathbf{v}_{2N_r-N_t}]$, the nulling process performs the linear operation

$$\check{\mathbf{y}}_n := \mathbf{V}^T\tilde{\mathbf{y}}_n = \mathbf{V}^T\tilde{\mathbf{H}}_{\Im}\Im\,\mathbf{s}_n + \mathbf{V}^T\tilde{\mathbf{w}}_n := \check{\mathbf{H}}_{\Im}\Im\mathbf{s}_n + \check{\mathbf{w}}_n$$

where $\check{\mathbf{H}}_{\Im}$ has dimension $(2N_r - N_t) \times N_t$ with real Gaussian independent identically distributed (i.i.d.) entries $\sim\mathcal{N}(\mathbf{0}, 1/2)$, and $\check{\mathbf{w}}_n \sim \mathcal{N}(\mathbf{0}, \|c_0\|^2 N_0/2\mathbf{I})$, since $\{\mathbf{v}_1, \mathbf{v}_2, \ldots, \mathbf{v}_{2N_r-N_t}\}$ is a set of orthonormal vectors. The real signal components from all the N_t transmit antennas are eliminated. With ML detection, we expect that the diversity order for the remaining symbols in $\Im\,\mathbf{s}_n$ is $N_r - N_t/2$. However, to reduce complexity, we will pursue suboptimal but simpler detectors.

Specifically, we will apply linear equalization to successive $\check{\mathbf{y}}_n$ vectors to reduce ISI in the imaginary components of the received signal. Even though the transmitted signals have the same power and ISI structure, due to independent fading, their instantaneous receive SNRs are different per receive antenna. This precludes application of linear MMSE equalization and motivates well linear zero-forcing (ZF) equalization. It has been tested that linear ZF equalization achieves essentially the same performance as linear minimum mean square error (MMSE) equalization for GMSK [7]. Let the $(2M+1)$-point ZF equalizer coefficients be $\{q_k\}_{k=-M}^{M}$. Then, the equalized vector becomes

$$\mathbf{r}_{2n} = \sum_{k=-M}^{M} q_k\check{\mathbf{y}}_{2n-2k} = \check{\mathbf{H}}_{\Im}\hat{\mathbf{a}}_{0,2n} + \hat{\mathbf{w}}_{2n} \tag{9}$$

where $\hat{\mathbf{a}}_{0,\,2n} := \sum_{k=-M}^{M} q_k\Im\,\mathbf{s}_{2n-2k}$ and $\hat{\mathbf{w}}_{2n} := \sum_{k=-M}^{M} q_k\check{\mathbf{w}}_{2n-2k}$. Vector $\hat{\mathbf{a}}_{0,\,2n}$ is the ZF estimate of the transmitted binary vector at time $2n$. ISI is reduced by linear equalization with small equalization loss. With perfect equalization, (9) becomes $\mathbf{r}_{2n} = \check{\mathbf{H}}_{\Im}\mathbf{a}_{0,2n} + \hat{\mathbf{w}}_{2n}$, where the entries of $\mathbf{a}_{0,2n}$ are drawn from $\{\pm 1\}$, and $\hat{\mathbf{w}}_{2n} \sim \mathcal{N}(\mathbf{0}, \|q\|^2\|c_0\|^2 N_0/2\mathbf{I})$. It is clear that with perfect equalization, the coded multiuser detection problem has been converted into an uncoded one.

We apply an efficient algorithm to solve the uncoded multiuser detection problem in a near-ML sense. There are several such algorithms known to solve this lattice search problem [1], [16]. In our simulation, we rely on sphere decoding (SD). It was reported in [6] that for a large range of SNR and any N_t, the *average* complexity of the SD is cubic. Further complexity reduction is possible with the Schnorr–Euchner variate of the SD algorithm [1]. Based on these facts, it follows that the average complexity of sphere decoding is $O\left(N_t^3\right)$.

Similar to the layered space–time systems [4], [14], the canceling process is as follows. Detected symbols are used to regenerate the imaginary components, which, in turn, are used to cancel the actual transmitted ones. With ideal canceling, the resulting signals contain only the transmitted real components and AWGN. The same low complexity linear ZF equalization and lattice search procedures can be applied to detect the symbols in the real components. Without error propagation and equalization loss, the detected symbols enjoy diversity order N_r, which is the full receive diversity. At this point, the transmitted symbols are all detected. However, it is possible that symbols carried by the real and imaginary parts have considerably different performance. This is suggested by the different diversity orders under ideal conditions. In fact, the overall BER performance is limited by the low diversity symbols.

To further improve performance, hard decision iterative decision feedback is applied. The detected symbols in the real components are used to regenerate and cancel the corresponding components from the original received signals, and symbols in the imaginary signal are detected again. This iterative process is applied repeatedly. Similar to most iterative decoders, simulations suggest that the performance gain is diminishing quickly. In many cases, two complete iterations are sufficient.

Let us now reflect on the pros and cons of combining sphere decoding with hard-decision iterative processing. It is known that the complexity of the SD algorithm is sensitive to the initial searching radius [6]. For the first iteration, the SD is the most computationally intensive block in the detection loop shown in Fig. 5. Nonetheless, in subsequent iterations, the SD solution of the last iteration can always serve as a high-quality estimate for the current one. In fact, it often coincides with the true solution. Based on this estimate, a distance upper bound can be determined and utilized as an initial sphere radius in the current search. With this appropriate radius, subsequent SD steps often exhibit considerably lower complexity. We conclude that the overall complexity for detecting symbols in one block is $O\left(N_t^3 N\right)$.

Relying on the special structure of MSK-type modulation, our LST-MSK design does not apply to general CPM. Nevertheless, the simplified Viterbi receivers in Section II-B can always be combined with conventional nulling-canceling detection or soft decision iterative decoding to obtain simplified LST-CPM receivers.

C. Performance Analysis of LST-MSK Receivers

The performance of our LST-MSK receiver is analyzed here. Since the LST-MSK receiver involves linear equalization and hard-decision iterative decoding, exact analysis is difficult, if not impossible. Several simplifying assumptions have to be made. The two-pulse approximation of a partial response MSK is assumed to be equivalent to the signal itself, since it is often the case that signal energy conveyed by the remaining pulses is negligible. Furthermore, no error propagation is assumed in the canceling process, which may not be true, in general. Nonetheless, received signals in our scheme are separated into only two component groups. Ideally, detected symbols enjoy a diversity order of at least $N_r - N_t/2$, which makes error propagation less severe when compared to conventional NC detection [4]. In fact,

our analytical results can always serve as an upper bound for the actual performance.

Since the detectors are identical for the real and imaginary groups, we only consider the imaginary group. With our simplifying assumptions, the signal from the νth transmit antenna is as follows:

$$s_\nu(t) = \sum_l a_{0,2l,\nu} c_0(t-2lT) + \sum_l a_{1,l,\nu} c_1(t-lT)$$

where the real symbol sequence $\{a_{0,2n-1,\nu}\}$ carried by $c_0(t)$ is perfectly eliminated. Because the symbol period in the imaginary arm is $2T$, matched filter outputs are sampled every $2T$ to obtain the decision statistics. At the μth receive antenna, these statistics are

$$y_{0,2n,\mu} = \sum_{\nu=1}^{N_t} h_{\mu,\nu} \sum_l a_{0,2l,\nu} \tilde{p}_{2n-2l} + \sum_{\nu=1}^{N_t} h_{\mu,\nu} \sum_l a_{1,l,\nu} \check{p}_{2n-l} + w_{2n,\mu}$$

where $\tilde{p}_n := \int c_0(t)c_0(t-nT)dt$, $\check{p}_n := \int c_1(t)c_0(t-nT)dt$, and $w_{n,\mu} := \int n_\mu(t)c_0(t-nT)dt$. For notational brevity, let us define

$$\zeta_n := \sum_{k=-M}^{M} q_k \tilde{p}_{n-2k}$$

$$\eta_n := \sum_{k=-M}^{M} q_k \check{p}_{n-2k}$$

$$\epsilon_{n,i} := \sum_{k=-M}^{M} q_k w_{n-2k,i}.$$

After linear ZF equalization, we obtain

$$r_{0,2n,\mu} = \sum_{k=-M}^{M} q_k y_{0,2n-2k,\mu} = \sum_{\nu=1}^{N_t} h_{\mu,\nu} \left[a_{0,2n,\nu} + a_{I,2n,\nu} \right] + \epsilon_{2n,\mu}$$

where $a_{I,2n,\nu} := \sum_{l,\, l\neq n} a_{0,2l,\nu}\zeta_{2n-2l} + \sum_l a_{1,l,\nu}\eta_{2n-l}$ is the remaining ISI from the νth transmit antenna. Collecting $r_{0,2n,\mu}$s in a vector $\mathbf{r}$ and dropping all subscripts for simplicity, we obtain

$$\mathbf{r} = \mathbf{H}(\,\mathbf{a} + \mathbf{a}_I\,) + \boldsymbol{\epsilon} \tag{10}$$

where $\mathbf{r}$ has dimension $N_r \times 1$ and $\boldsymbol{\epsilon} \sim \mathcal{CN}(\mathbf{0}, ||q||^2||c_0||^2 N_0 \mathbf{I})$. In this vector model, $\mathbf{a}$ is the transmitted vector at time $2n$, and $\mathbf{a}_I$ is the remaining ISI after equalization.

To identify performance-affecting factors, we focus on the pairwise error probability (PEP) next. The conditional PEP between two transmitted vectors $\mathbf{a}$ and $\mathbf{a}'$ is calculated first. Let $\mathbf{h} := \mathbf{H}(\mathbf{a}-\mathbf{a}')$. Then, the conditional PEP is

$$P(\mathbf{a}\to\mathbf{a}'|\mathbf{h}) = P(||\mathbf{h}||^2 + 2\Re\left\{\mathbf{h}^H\left[\mathbf{H}\mathbf{a}_I + \boldsymbol{\epsilon}\right]\right\} < 0 | \mathbf{h}). \tag{11}$$

Due to the residual ISI vector $\mathbf{a}_I$, even the exact PEP expression is difficult to obtain. However, simple upper and lower bounds can be derived. Define two additional vectors $\mathbf{a}_1$ and $\mathbf{a}_2$ as follows. If $\mathbf{a}(i) \neq \mathbf{a}'(i)$, then $\mathbf{a}_1(i) := \mathbf{a}_I(i)$; otherwise, $\mathbf{a}_1(i) := 0$. Conversely, if $\mathbf{a}(i) = \mathbf{a}'(i)$, then $\mathbf{a}_2(i) := \mathbf{a}_I(i)$; otherwise, $\mathbf{a}_2(i) := 0$. It follows that $\mathbf{a}_I = \mathbf{a}_1 + \mathbf{a}_2$. The residual ISI symbols in $\mathbf{a}_I$ are assumed deterministic but unknown. Using the Cauchy–Schwarz inequality, it can be shown that

$$-k||\mathbf{h}||^2 \le \mathbf{h}^H\mathbf{H}\mathbf{a}_1 \le k||\mathbf{h}||^2 \tag{12}$$

where $k = (\sum_{l,\, l\neq n}|\zeta_{2n-2l}| + \sum_l |\eta_{2n-l}|)/2$. It can also be inferred that $\mathbf{H}\mathbf{a}_2$ is zero mean complex Gaussian distributed and independent to $\mathbf{h}$. That is,

$$\mathbf{h}^H\mathbf{H}\mathbf{a}_2 \sim \mathcal{CN}(0,\sigma^2), \quad 4k_0^2 N_c||\mathbf{h}||^2 < \sigma^2 < 4k^2 N_c||\mathbf{h}||^2 \tag{13}$$

where N_c is the number of positions where the corresponding symbols in $\mathbf{a}$ and $\mathbf{a}'$ agree, and $k_0 := (|\nu_0| - \sum_{l,l\neq n}|\mu_{2n-2l}| - \sum_{l,l\neq 2n}|\nu_{2n-l}|)/2$. Applying (12) and (13) to (11), the upper and lower bounds for the conditional PEP are

$$\mathcal{Q}(k_1||\mathbf{h}||\mathbf{h}) < P(\mathbf{a}\to\mathbf{a}'|\mathbf{h}) < \mathcal{Q}(k_2||\mathbf{h}||\mathbf{h}) \tag{14}$$

where $k_1 := (1+2k)/\sqrt{8k_0^2N_c + 2||q||^2||c_0||^2N_0}$, and $k_2 := (1-2k)/\sqrt{8k^2N_c + 2||q||^2||c_0||^2N_0}$. Let $N_e := N_t - N_c$ be the number of corresponding symbols that $\mathbf{a}$ and $\mathbf{a}'$ differ. Based on our channel model, $||\mathbf{h}||^2$ follows a central Chi-square probability density function

$$p(x) = \frac{1}{(4N_e)^{N_r}(N_r-1)!}x^{N_r-1}\exp\left(-\frac{x}{4N_e}\right), \quad x \ge 0.$$

Exact unconditional expressions for the bounds in (14) can be derived; see, e.g.,[12, p. 103]. To gain further insight, the Chernoff bound $\mathcal{Q}(x) < \exp(-x^2/2)/2$ is sufficient. The PEP upper bound is

$$P(\mathbf{a}\to\mathbf{a}') < \frac{\left(2N_e k_2^2 + 1\right)^{-N_r}}{2}. \tag{15}$$

At this point, several observations can be made.

1) For perfect equalization, $k = 0$. Following the definition of k_2 and (15), it is clear that PEP enjoys full receive diversity. Furthermore, all pairwise errors enjoy the same diversity order N_r but have different coding advantages due to different N_es in (15).
2) Theoretically, error floor shows up at high SNR. This is because both k_1 and k_2 approach some nonzero constants as N_0 approaches zero, when $k > 0$. However, with small equalization loss, error floor does not appear for practical SNR values.
3) Tighter upper and lower bounds for the conditional PEP can be derived by averaging out the strongest residual ISI symbols in $\mathbf{a}_I$ and bounding the remaining symbols deterministically.
4) Even though asymptotically pessimistic, our LST-MSK receivers exhibit considerable performance improvement relative to conventional nulling-canceling detectors.

IV. Simulations

The performance of our LST-MSK receiver is tested here by Monte Carlo simulations. The transmitted signals are generated according to the classical CPM representation (1). Since our concern is on bandwidth efficient CPM, partial response GMSK is utilized in our simulations with spectral shaping pulse [2]

$$g(t) = \frac{1}{T}\left[\mathcal{Q}\left(c\left(t-\frac{T}{2}\right)\right) + \mathcal{Q}\left(c\left(t+\frac{T}{2}\right)\right)\right]$$
$$c = \frac{2\pi B}{\sqrt{\ln 2}}$$

where B denotes the 3-dB bandwidth, and the duration of $g(t)$ is truncated to $L = 4$. Partial response GMSK with $BT = 0.25$ is employed. The continuous signal generation and matched filtering are implemented with discrete-time equivalent operations. To avoid aliasing, up-sampling and down-sampling operations are implemented.

Example 1: An LST-MSK receiver with a five-tap real linear ZF equalizer $(M = 2)$ is employed. The performance for a system with $N_t = 8$ transmit and $N_r = 8$ receive antennas is shown in Fig. 6, where error performance of the symbols carried by the real and imaginary components of the transmitted signals are shown separately. The overall performance is limited by the group of symbols with the worst performance. To boost the overall performance, hard-decision iterative canceling is employed. We observe that the performance gain for the second iteration is the most noticeable. This gain diminishes quickly with additional iterations. In many cases, we found that two (or even one and a half) iterations are sufficient to exploit the performance gain of the hard decision iterative detection.

To benchmark performance, two additional curves are plotted in Fig. 6. The first curve shows the performance of the conventional LST receiver employing NC with optimal detection ordering [18]. Only the performance of the first detected layer is shown, since the overall performance is dominated by this layer. After determining the optimal detection order, signals from undesired transmitters are eliminated by nulling, and a simplified four-state Viterbi receiver is employed to detect the symbols from the desired transmitter. The performance gain of our LST-MSK receiver is noticeable, which is not unexpected since the conventional NC decoder does not fully exploit the receive diversity. The second curve corresponds to the performance of symbols carried by the real component group with perfect elimination of the imaginary group. This can serve as an upper bound for the performance of our LST-MSK receiver. More accurately, it may be even better than the ML performance of LST-MSK, since performance loss due to linear equalization in each group is relatively small, and interference from one component group is perfectly eliminated.

Example 2: Performance of our LST-MSK receiver for a four-transmit and four-receive antennas system is shown in Fig. 7. In the same figure, performance of a receiver with direct linear ZF equalization followed by an SD algorithm is also depicted. For the latter, a ZF equalizer with nine complex taps $(M = 4)$ is employed. Due to the severe ISI, direct application of linear equalization causes large equalization loss. It is clear from Fig. 7 that this performance loss is considerable.

Example 3: To simplify the performance analysis of the LST-MSK receiver, we have assumed perfect canceling of the detected symbols. In general, this assumption is not corroborated fully by our simulations. Error propagation does exist. We can observe this effect from both Figs. 6 and 7. There are gaps between the performance of the hard-decision iterative decoding and those of perfect canceling. However, we have observed that in other simulations, the perfect canceling performance is closely approached by our LST-MSK receiver. In Fig. 8, the performance of an LST-MSK system with $N_t = 2$ and $N_r = 4$ is shown. We observe that perfect NC performance is achieved with the second iteration. We encountered similar examples frequently when $N_t < N_r$.

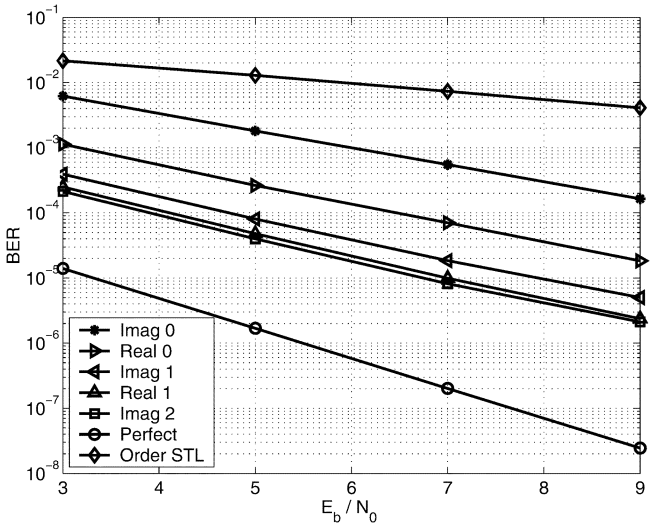

Fig. 6. Performance comparison of the LST-MSK receiver versus conventional LST nulling-canceling receiver with optimal detection ordering for $N_t = N_r = 8$.

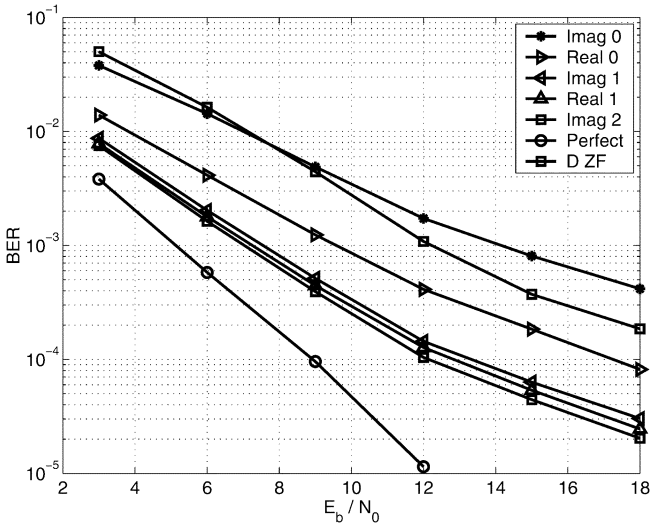

Fig. 7. Performance comparison of the LST-MSK receiver versus the direct ZF equalization and sphere decoding for $N_t = N_r = 4$

V. Conclusion

ML receiver complexity for an LST system with a large number of transmit and receive antennas is, in general, very high. ST systems employing CPM are motivated by their high bandwidth and power efficiency. However, the high-decoding complexity renders the already complex ST detection even

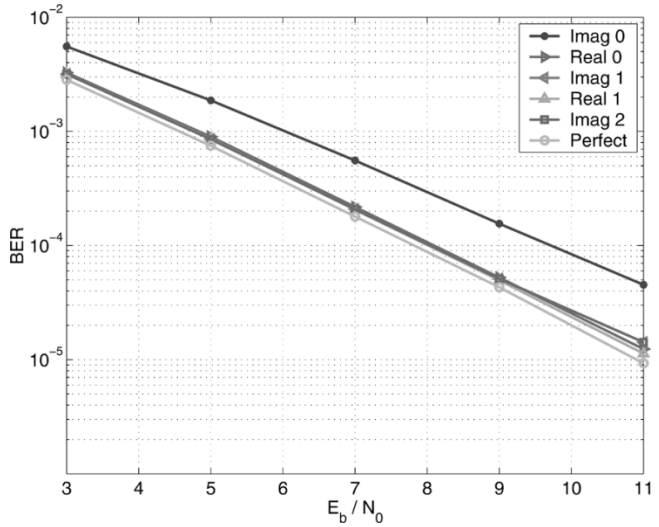

Fig. 8. LST-MSK design example without severe error propagation for $N_t = 2$ and $N_r = 4$.

worse. In this paper, we developed reduced complexity receiver designs for multiantenna LST systems with binary CPM.

For single-antenna binary CPM, we explicitly derived the minimum trellis of the simplified Viterbi receivers. Based on this design, differential encoding was introduced for the special class of CPM signals with $h = 1/(2Q)$, $Q \in \mathbb{N}$. The resulting performance gains were justified both theoretically and with simulations.

For multiantenna systems, we designed reduced complexity LST-MSK receivers. With group nulling-cancelling and linear ZF equalization, we converted a coded multiuser detection problem into an uncoded one with low complexity and small performance loss. Then, we applied the efficient SD algorithm to solve this problem. To improve performance, we also employed hard-decision iterative decoding. The combination of SD with iterative decoding turned out to be effective in boosting performance with a controllable complexity increase. With both theoretical analysis and Monte Carlo simulations, we established that our LST-MSK receiver exhibits improved performance with moderate complexity.

REFERENCES

[1] E. Agrell, T. Eriksson, A. Vardy, and K. Zeger, "Closest point search in lattices," *IEEE Trans. Inf. Theory*, vol. 48, no. 8, pp. 2201–2214, Aug. 2002.

[2] J. B. Anderson, T. Aulin, and C. E. Sundberg, *Digital Phase Modulation* New York, Plenum, 1986.

[3] J. Boutros and G. Caire, "Iterative multiuser joint decoding: Unified framework and asymptotic analysis," *IEEE Trans. Inf. Theory*, vol. 48, no. 7, pp. 2201–2214, Jul. 2002.

[4] G. J. Foschini, "Layered space–time architecture for wireless communication in a fading environment when using multielement antennas," *Bell Labs. Tech. J.*, vol. 1, no. 2, pp. 41–49, Autumn 1996.

[5] G. J. Foschini and M. J. Gans, "On limits of wireless communication in a fading environment when using multiple antennas," *Wireless Personal Commun.*, vol. 6, no. 3, pp. 311–335, Mar. 1998.

[6] B. Hassibi and H. Vikalo, "On the expected complexity of sphere decoding," in *Proc. 35th Asilomar Conf. Signals, Systems, Computers*, Pacific Grove, CA, Nov. 2001, pp. 1051–1055.

[7] G. Kaleh, "Simple coherent receivers for partial response continuous phase modulation," *IEEE Trans. Sel. Areas Commun.*, vol. 7, no. 9, pp. 1427–1436, Dec. 1989.

[8] P. Laurent, "Exact and approximate construction of digital phase modulations by superposition of amplitude modulated pulses (AMP)," *IEEE Trans. Commun.*, vol. 34, no. 2, pp. 150–160, Feb. 1986.

[9] U. M. Morelli, "Decomposition of M-ary CPM signals into PAM waveforms," *IEEE Trans. Inf. Theory*, vol. 41, no. 5, pp. 1265–1275, Sep. 1995.

[10] J. Proakis, *Digital communications*, 3rd ed. New York: McGraw-Hill, 1995.

[11] B. Rimoldi, "A decomposition approach to CPM," *IEEE Trans. Inf. Theory*, vol. 34, pp. 260–270, Mar. 1988.

[12] M. K. Simon and M. S. Alouini, *Digital Communication Over Fading Channels*. New York: Wiley, 2000.

[13] G. Stüber, *Principles of Mobile Communication*, 2rd ed. Boston, MA: Kluwer, 2000.

[14] V. Tarokh, A. Naguib, N. Seshadri, and A. R. Calderbank, "Combined array processing and space–time coding," *IEEE Trans. Inf. Theory*, vol. 45, no. 4, pp. 1121–1128, May 1999.

[15] I. E. Telatar, "Capacity of multi-antenna Gaussian channels," *Eur. Trans. Telecommun.*, vol. 10, no. 6, pp. 585–595, Nov. 1999.

[16] E. Viterbo and J. Boutros, "A universal lattice code decoder for fading channels," *IEEE Trans. Inf. Theory*, vol. 45, no. 5, pp. 1639–1642, Jul. 1999.

[17] G. Wang and X.-G. Xia, "Orthogonal space–time coding for CPM system with fast decoding," in *Proc. Int. Conf. Communications*, vol. 3, New York, Apr. 2, 2002, pp. 1788–1792.

[18] P. W. Wolniansky, G. J. Foschini, G. D. Golden, and R. A. Valenzuela, "V-BLAST: An architecture for realizing very high data rates over the rich-scattering wireless channel," in *Proc. ISSSE*, Pisa, Italy, Sep. 1998.

[19] X. Zhang and M. Fitz, "Soft-output demodulator in space–time coded continuous phase modulation," *IEEE Trans. Signal Process.*, vol. 50, no. 10, pp. 2589–2598, Oct. 2002.

[20] ——, "Space–time code design with CPM transmission," in *Proc. Int. Symp. Information Theory*, Washington, DC, Jun. 24–29, 2001, pp. 237–237.

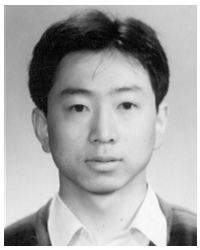

Wanlun Zhao (S'02) received the B.S. degree in electrical engineering and information science from the Huazhong University of Science and Technology (HUST), Wuhan, China, in June 1996, and the M.Sc. degree in applied mathematics from the University of Minnesota, Minneapolis, in 2000. He is currently working toward the Ph.D. degree in the Department of Electrical and Computer Engineering, University of Minnesota.

His research interests include the areas of wireless communication and coding techniques.

Georgios B. Giannakis (S'84–M'86–SM'91–F'97) received the Diploma in electrical engineering from the National Technical University of Athens, Greece, in 1981, and the M.Sc. degree in electrical engineering, the M.Sc. degree in mathematics, and the Ph.D. degree in electrical engineering, all from the University of Southern California (USC), Los Angeles, in 1983 and 1986, respectively.

After lecturing for one year at USC, he joined the University of Virginia in 1987, where he became a Professor of electrical engineering in 1997. Since 1999, he has been a Professor with the Department of Electrical and Computer Engineering, University of Minnesota, Minneapolis, where he now holds an ADC Chair in Wireless Telecommunications. His general interests span the areas of communications and signal processing, estimation and detection theory, time-series analysis, and system identification—subjects on which he has published more than 200 journal papers, 350 conference papers, and two edited books. His current research interests include transmitter and receiver diversity techniques for single- and multiuser fading communication channels, complex-field and space–time coding, multicarrier, ultrawide-band wireless communication systems, cross-layer designs, and distributed sensor networks.

Dr. Giannakis is the (co-)recipient of six paper awards from the IEEE Signal Processing (SP) and Communications Societies (1992, 1998, 2000, 2001, 2003, 2004). He also received the SP Society's Technical Achievement Award in 2000. He served as Editor-in-Chief for the IEEE SIGNAL PROCESSING LETTERS, as Associate Editor for the IEEE TRANSACTIONS ON SIGNAL PROCESSING and the IEEE SIGNAL PROCESSING LETTERS, as Secretary of the SP Conference Board, as member of the SP Publications Board, as member and Vice Chair of the Statistical Signal and Array Processing Technical Committee, as Chair of the SP for Communications Technical Committee, and as a member of the IEEE Fellows Election Committee. He has also served as a member of the the IEEE-SP Society's Board of Governors, the Editorial Board for the PROCEEDINGS OF THE IEEE, and the steering committee of the IEEE TRANSACTIONS ON WIRELESS COMMUNICATIONS.